Journal of Biomolecular NMR, **23:** 23–33, 2002.
KLUWER/ESCOM

Practical aspects of the 2D ^{15}N-{^{1}H}-NOE experiment

Christian Renner[a,*], Michael Schleicher[b], Luis Moroder[a] & Tad A. Holak[a]
[a]*Max-Planck-Institut für Biochemie, 82152 Martinsried, Germany;* [b]*Ludwig-Maximilians-Universität, Adolf-Butenandt-Institut, 80336 München, Germany*

Received 20 December 2001; Accepted 29 January 2002

Key words: heteronuclear NOE, high resolution NMR, ^{15}N relaxation, protein dynamics

Abstract

The heteronuclear ^{15}N-NOE experiment was extensively tested with respect to statistical and systematic experimental error. The dependence of signal intensity in the NOE experiment and in the reference experiment on the saturation and relaxation time was experimentally investigated. The statistics of the experimental values were accessed by numerous repetitions of identical set-ups. As a model system a protein of typical size for NMR studies was chosen, i.e., a 120 amino acid residues containing fragment of the F-actin binding gelation factor (ABP-120). The fragment exhibits fast dynamics that are accessible with the ^{15}N-NOE experiment with various amplitudes. The results of this study show that commonly used parameters are only adequate for accurate measurement of motions with moderate amplitude. Highly flexible parts require longer delay times and thus more experimental time than commonly used. On the other hand, a qualitative or semi-quantitative assessment of a protein's mobility on fast times scales can be obtained from rapidly recorded experiments with unusual short delay times. The findings of this study are of equal importance for highly accurate measurement of the ^{15}N-NOE as well as for quick identification of mobile or even unstructured residues/parts of a protein.

Introduction

One of the strengths of NMR is its ability to study the dynamic behaviour of proteins under almost physiological conditions, i.e., in aqueous solution, and at an atomic level (Dayie et al., 1996; Palmer, 1997; Kay, 1998; Fischer et al., 1998). The heteronuclear two-dimensional ^{15}N-{^{1}H} nuclear Overhauser effect (hetNOE) is the most universally used NMR experiment to access protein dynamics on fast time scales (ps – ns). It allows quantification of thermal fluctuations in a protein on a per residue basis (Kay et al., 1989; Clore et al., 1990; Peng and Wagner, 1992; Orekhov et al., 1995; Zheng et al., 1995; Fushman et al., 1997; Renner et al., 1998). Partially flexible parts, such as surface exposed loops, are readily distinguished from the folded core (Zink et al, 1994; Lefèvre et al., 1996; Papavoine et al., 1997; Renner et al., 2001). Unstructured parts or unfolded proteins frequently yield signals of opposite sign and can thus be recognized on first glance (Buck et al., 1996; Fucini et al., 1997; Mühlhahn et al., 1998; Viles et al., 2001). In this respect the hetNOE experiments can be useful in all stages of a protein NMR study: quantification of unfolded residues in protein candidates for structure elucidation, cross-validation between secondary structure assignment and hetNOE value, correlation between ill-defined parts of a structure family and reduced hetNOE values, and finally characterization of protein dynamics.

The drawback of the hetNOE experiment is its low inherent sensitivity. At the beginning of the pulse sequence one starts with the equilibrium ^{15}N magnetization instead of the equilibrium ^{1}H magnetization that is approx. tenfold stronger and used for other relaxation measurements such as T_1, T_2 relaxation or CSA-dipole dipole cross correlation measurements (Farrow et al., 1994; Tjandra et al., 1996; Tessari et al., 1997; Fushman et al., 1999). The only possibility to reduce the experimental time for a given sample and to

*To whom correspondence should be addressed.
E-mail: renner@biochem.mpg.de

achieve a desired signal to noise ratio is an increase of the scan repetition rate, that is a decrease of the relaxation delay. However, it is known that short relaxation delays lead to systematic errors in the hetNOE values (Smith et al., 1987; Kay et al., 1989; Clore et al., 1990; Grzesiek and Bax, 1993; Skelton et al., 1993; Li and Montelione, 1994). Especially chemical exchange of amide protons with saturated water protons was shown to artificially increase hetNOE ratios (Grzesiek and Bax, 1993; Skelton et al., 1993; Li and Montelione, 1994). In two previous studies theoretical predictions were given for the dependence of the measured hetNOE on the relaxation delay (Skelton et al., 1993; Li and Montelione, 1994). However, experimentally only few hetNOE experiments were performed with long relaxation delays between 4 s and 15 s. The dependence of the measured hetNOE values on the length of the saturation period was not investigated.

In this study systematic errors in the hetNOE experiment were experimentally mapped for different degrees of mobility corresponding to highly structured and almost completely disordered parts of proteins. A protein fragment from the F-actin binding gelation factor (ABP-120) with a rigid folded core (IG-fold) and an unstructured C-terminal tail (Fucini et al., 1997) was chosen as model system for simultaneous mapping of amino acid residues with low, medium and high flexibility. The folded core (segment 4 of the rod domain of the gelation factor) is very rigid, as expected for the immunoglobulin fold, whereas the last 20 residues at the C-terminus are completely unstructured. Between folded core and unstructured tail mobility gradually increases. The dependence of systematic errors on the relaxation delay and on the saturation period are investigated experimentally and compared to theory and simulation, respectively. Parameter sets are derived for highly accurate NOE measurements as well as for quick qualitative assessment of the dynamics of a protein.

Experimental

HetNOE measurements

NMR experiments were carried out at 31° on a BRUKER AMX500 spectrometer equipped with PFG accessories on a 1.5 mM uniform ^{15}N-labeled sample of segment 4 of the gelation factor (ABP 120) in 90% H_2O/10% D_2O at pH 7.0. The construct of the gelation factor used in this study comprises 122 residues (Fucini et al., 1997). Residues 1-100 are folded and constitute the proper 4th segment of the rod domain of the gelation factor. The C-terminal 22 residues are unfolded (Fucini et al., 1997). Modified versions of the experiments proposed by Farrow et al. (1994) were used for the ^{15}N-{^{1}H} heteronuclear NOE and the reference experiment. To avoid saturation of the water resonance a rectangular low power 2 ms water flip-back pulse was employed (Grzesiek and Bax, 1993). 140 times 2048 data points were recorded with a spectral width of 35 ppm (^{15}N) and 11 ppm (^{1}H), respectively. Saturation of the amide protons in the heteronuclear NOE experiment was achieved by the application of a series of 120° pulses prior to the experiment (Markley et al., 1971). In all cases the scan repetition rate was equal for NOE and reference experiment, i.e. relaxation delay plus saturation delay in the NOE experiment equals relaxation delay in the reference experiment. Table 1 summarizes the delays that were used and the number of identical experiments that were performed for each set. Altogether 24 sets of NOE and reference experiments were acquired. With 1–2 days measurement time per experiment in total two months of pure instrument time were used. Spectra were processed and analysed with CCNMR (Cieslar et al., 1993). NOE values are given simply by the ratio of the peak heights in the experiment with and without proton saturation. Statistical analysis was programmed in C programming language and tested with random numbers (with Gaussian distribution). The Nth moment (N = 1, 2, 3, 4, 5, 6) (Bronstein and Semendjajew, 1957) was calculated for amino acids 1 to 100 (folded core) from eight repetitions of the same hetNOE set-up (3 s saturation delay, 5 s relaxation delay). Mean value and standard deviation of the Nth moment for residues 1–100 were determined.

Investigation of relaxation and saturation in hetNOE measurements

Experiments for systematic mapping of relaxation and saturation behaviour in the NOE experiment were recorded on a Bruker DRX500 spectrometer using the same sample and the same temperature (31°) as above. T_1 of water was measured with 1D inversion recovery experiments employing gradients during the recovery period to prevent radiation damping. Signal integrals were proportional to $1–2 \times \exp(-t_r/T_1)$ over the whole range of recovery times t_r (between 0.1 s and 8 s) with $T_1 = 3.4$ s.An average proton T_1 was also measured by 1D inversion recovery. Sig-

Table 1. Relaxation and saturation delays of hetNOE experiments

Relaxation delay in reference experiment	12 s	8 s	5 s	5 s	3.1 s	1.6 s
Saturation delay in NOE experiment[a]	3 s	3 s	3 s	1 s	3 s	1.5 s
Number of measurements with identical set-up	2	2	8	3	3	6

[a]The relaxation delay preceding the saturation time in the NOE experiment is relaxation delay in the reference experiment minus saturation delay of the NOE experiment to keep the scan repetition rate constant.

nals downfield from 8.5 ppm were used to obtain a $T_1 = 1.3$ s for amide protons in the structured part. The fraction of water magnetisation preserved in the water flip-back version of the NOE reference experiment was determined as follows: at the end of the normal NOE reference experiment a small angle water readout pulse was appended and the experiment was performed in a one-dimensional manner (= the first t_1 increment). Simultaneous phase cycling (0°, 180°) of the read-out pulse and the receiver was used to suppress the protein signal that is normally detected in the NOE reference experiment. The relaxation delay was set to 20 s to ensure full relaxation of the water magnetisation between scans. This experiment was performed once with all pulses and parameters as in the real NOE reference experiment and once with all proton pulses (except the readout pulse) disabled. The ratio of the former to the later is the fraction of water magnetisation preserved in the NOE reference experiment with water flip-back pulse. Different readout pulses (0.1 μs at 0 dB rect., 1 μs at 36 dB rect., 100 μs at 60 dB sinc), all corresponding to a total rotation of less than 1°, gave the same result (80% of water magnetisation left at the beginning of the signal acquisition). Performing this experiment with either the water flip-back pulse or the read-out pulse disabled resulted in no signal, as expected.

The relaxation in the NOE reference experiment was mapped in a pseudo 2D experiment by recording the first t_1 increment for various relaxation delays between 10 ms and 20 s. 512 scans and small steps of the relaxation delay were used to ensure an equilibrium situation for each value for the relaxation delay. Amide signals above 8.5 ppm and between 8.5 and 8.1 ppm were integrated to yield information on the rigid and flexible residues, respectively. Additionally, full 2D hetNOE reference experiments were recorded with relaxation times of 1.6 s, 3 s, 5 s, 8 s and 12 s. Signals from the middle of the unfolded C-terminal tail (Gly-110 and Gly-112) were averaged as an example for unstructured residues. For rigid residues from the folded core data from full 2D and from pseudo 2D experiments agreed very well, thereby confirming the correctness of the pseudo 2D approach. In general, with the Bruker DRX spectrometer console reproducibility of experiments was found to be very good. Spectra with identical set-up recorded several days apart were always identical down to the noise level. It might therefore be preferable to record NOE reference and saturation experiment sequentially, because in the interleaved mode one switches between fully saturating and largely relaxing magnetisation, especially water magnetisation. This can cause small transient changes in the saturation/relaxation state of (water) magnetisation at the beginning of a t_1 increment.

The dependence of the signal on the length of the saturation period was investigated in the NOE saturation experiment in a similar manner as for the reference experiment. Saturation periods between 10 ms and 8 s were used. The saturation period was preceded by a relaxation delay of either 100 ms or 1 s. No water flip-back pulse was applied in this saturation experiments. To test saturation of the water magnetisation during the saturation period, separate pseudo 2D experiments consisting only of the saturation period and a final 90° hard pulse were performed. To monitor saturation of protein proton magnetisation, the WATERGATE sequence was appended. Again relaxation delays of 100 ms or 1s preceded the saturation period. In all saturation experiments saturation was achieved by equally spaced pulse trains. Three different flip angles for these pulses were tested for all saturation experiments described above: the commonly used 120° (Kay et al., 1989; Clore et al., 1990; Farrow et al., 1994; Zink et al., 1994; Renner et al., 1998; Mühlhahn et al., 1998; Viles et al., 2001), 188°, newly proposed in this paper (the odd value of 188° has no special meaning but corresponds to the round value of 24 μs that was used as pulse length), and the original 250° proposed by Markley et al. (1971). In the simple proton saturation experiments different pulse spacings of 5 ms, 10 ms and 20 ms were used, whereas in the NOE saturation experiment only pulse trains with 10 ms spacing were employed. All test spectra were

processed and analysed with XWINNMRv3.0 (Bruker Biospin, Karlsruhe, Germany) and results were plotted with GNUPLOT.

Simulations

Saturation of proton magnetisation with equally spaced pulse trains was simulated for isolated spins using NMRSIMv3.0 (Bruker Biospin, Karlsruhe, Germany). The full relaxation approach taking into account T_1 and T_2 relaxation during the pulse sequence and the acquisition time was used with $T_1 = T_2 = 3.4$ s for simulation of water protons and $T_1 = 1.3$ s and $T_2 = 40$ ms for simulation of protein amide protons. The chemical shift offset for the simulations shown here was set to zero, but in additional simulations the final saturation levels for very long saturation times were found to be independent of the offset (within reasonable limits). Radiation damping is not included in the simulations. The set-up of the simulations was essentially identical to the simple proton saturation experiments for water described in the previous section, i.e., without WATERGATE. Analogous to the NMR experiments, different flip angles (120°, 180° and 250°) were used for the saturation sequence with a constant spacing of 10 ms.

Results and discussion

HetNOE measurements

Figure 1 shows the NOE values that are obtained with different relaxation and saturation delays. For the rigid residues of the folded core all curves agree nicely except for the shortest saturation delay (1 s) and the shortest relaxation delay (1.6 s) where the NOE value is overestimated by 14% and 19%, respectively. All relaxation delays longer than 3 s yielded the same intensities within experimental error. However, for the flexible unstructured C-terminus there is even a marked difference between relaxation delays as long as 8 s and 12 s. It should be kept in mind that as long as the NOE value is positive, insufficient saturation as well as insufficient relaxation leads to NOE values that are larger than the true NOE. Therefore, in cases of limited flexibility the NOE values obtained with very short delay times are upper limits to the true values. For flexible amino acids with small or negative NOE values the situation is much worse. The shortest relaxation delay yields completely unphysical NOE values (Figure 1, inset). For the other delay times NOE values become less negative with increasing delay length. Only relaxation delays of 5 s or longer produce meaningful NOE values for all mobile residues. Interestingly, for negative NOEs incomplete relaxation and incomplete saturation can partially cancel each other as demonstrated in Figure 1 by the NOE ratios of very flexible residues (box on the right hand side) obtained with 1 s saturation/5 s relaxation (yellow curve) that agree well with the NOE ratios using the longest relaxation delay (12 s, black curve).

Statistics

To investigate the statistical error in the hetNOE experiment eight sets of NOE and reference experiments with identical relaxation and saturation delays (5 s/3 s) were recorded. With these delay times only NOE values of residues with restricted mobility can be measured accurately (see above). Therefore, only NOE values of residues belonging to the folded part of the protein (1–100) were used for the further calculations. For each amino acid the 1st moment (= average), 2nd moment (= variance), 3rd, 4th, 5th and 6th moment were calculated (Bronstein and Semendjajew, 1957). For each moment the average over all residues as well as the standard deviation was determined. The 4th moment of a Gaussian distribution equals three times the square of the 2nd moment. Here a mean 2nd moment of 0.9938×10^{-3} with a standard deviation of 0.6579×10^{-3} was found. The 4th moment with a mean of 3.8363×10^{-6} and a standard deviation of 8.1659×10^{-6} is compatible with a Gaussian distribution ($3 \times (\text{2nd moment})^2 = 3 \times 10^{-6}$), however, due to the large standard deviation it is not significant. The fact that for all higher moments (3rd to 6th) mean values are much smaller than the standard deviations does not allow to prove the Gaussian character of the distribution, but allows to conclude that the distribution is neither asymmetric nor broader than a Gaussian distribution to detectable extents. The variance calculated from N samples (here N = 8) is related to the variance of the distribution (calculated with an infinite number of samples) as Var(N) = Var(inf) (N – 1)/N. Therefore, Var(inf) = 8/7 times Var(8) = $1.143 \times 0.9938 \times 10^{-3}$ = 0.001136 = $(3.4\%)^2$. The mean standard deviation for the distribution of NOE values (= experimental statistical error) is therefore 3.4%. Common practice is to calculate this standard deviation as RMSD between two measurements with identical set-up. Calculating the RMSD for all pairs of measurements (eight measurements = 28 pairs) and then averaging all 28

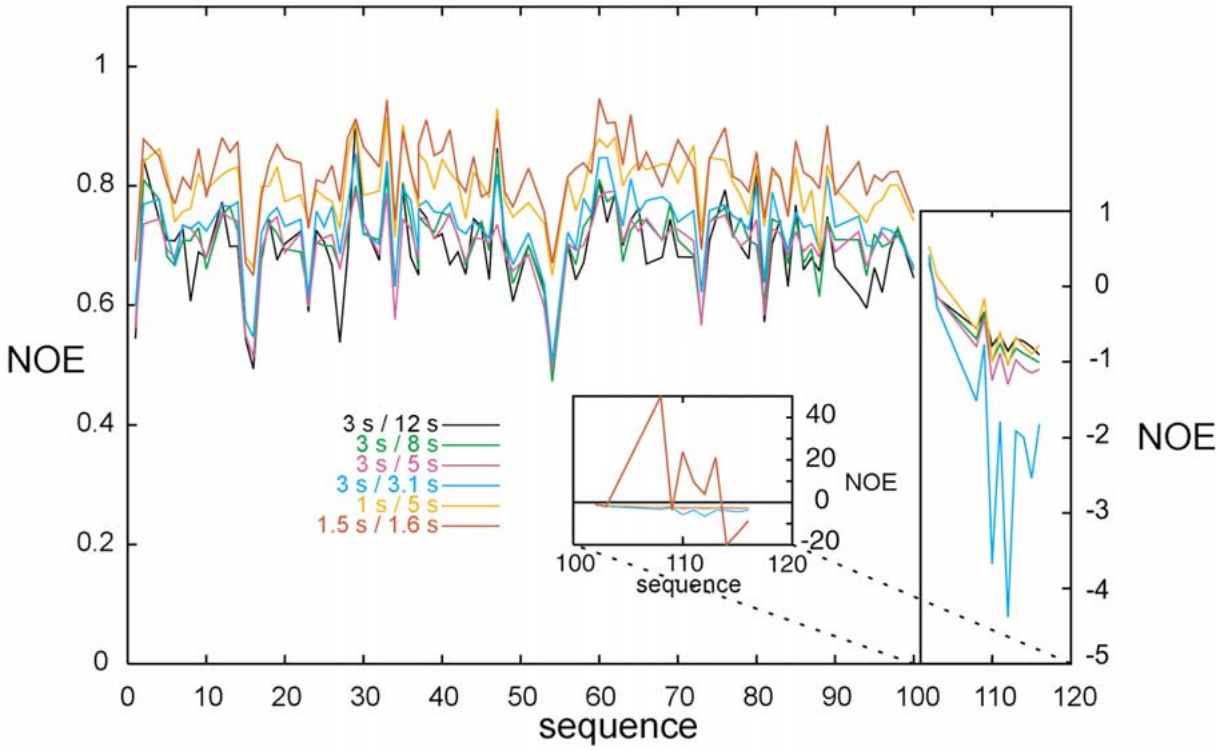

Figure 1. NOE values for different scan repetition rates measured at 31° and 500 MHz. For each curve the saturation time in the NOE experiment with proton saturation as well as the relaxation time in the NOE reference experiment is given (sat. time/relax. time). Note the different scales on the ordinate for the different boxes.

RMSDs results in an estimated statistical error of 4% in good agreement with the 3.4% obtained above. All RMSDs were in the range from 3.3% to 5% so that the RMSD method seems quite robust. The error estimation from double recordings contains not only the thermal noise in the spectrum, but also fluctuations in experimental conditions such as instabilities of temperature, amplifiers, electronics etc., which have to be considered statistically as their effects can usually not be determined separately. However, one obtains only an average error for all signals. When individual error estimates are required, e.g., error bars in a plot, it is important not to use the standard deviation calculated from the two measured values, but to calculate the individual absolute error by multiplying the individual (mean) value with the average relative error. This is a good estimate as long as peak intensities are similar for all signals. Note that estimating the experimental error from noise in the spectra, another popular method, yields only a lower limit of the experimental error.

Saturation in the NOE experiment with proton saturation

To investigate the saturation behaviour in the NOE saturation experiment, saturation of proton magnetisation was directly measured as a function of saturation time and using different pulse trains for the saturation period. For broadband saturation of proton magnetisation we tested the commonly used 120° pulses as well as 250° pulses as originally proposed by Markley et al. (1971). Additionally, a stepwise increase of the pulse length in the saturation period for a constant overall saturation time indicated that approximate 180° pulses might perform even better than the known saturation sequences. Therefore we performed all saturation tests also with 188° saturations pulses (188° corresponded to 24 μs pulse length). Figure 2 shows the saturation curves obtained for water and for protein magnetisation. In both cases the saturation period was preceded by a 1 s relaxation delay. Simulations analogous to the NMR measurements were performed on an isolated proton spin and compared to the experimental curves. The large differences between experiment and

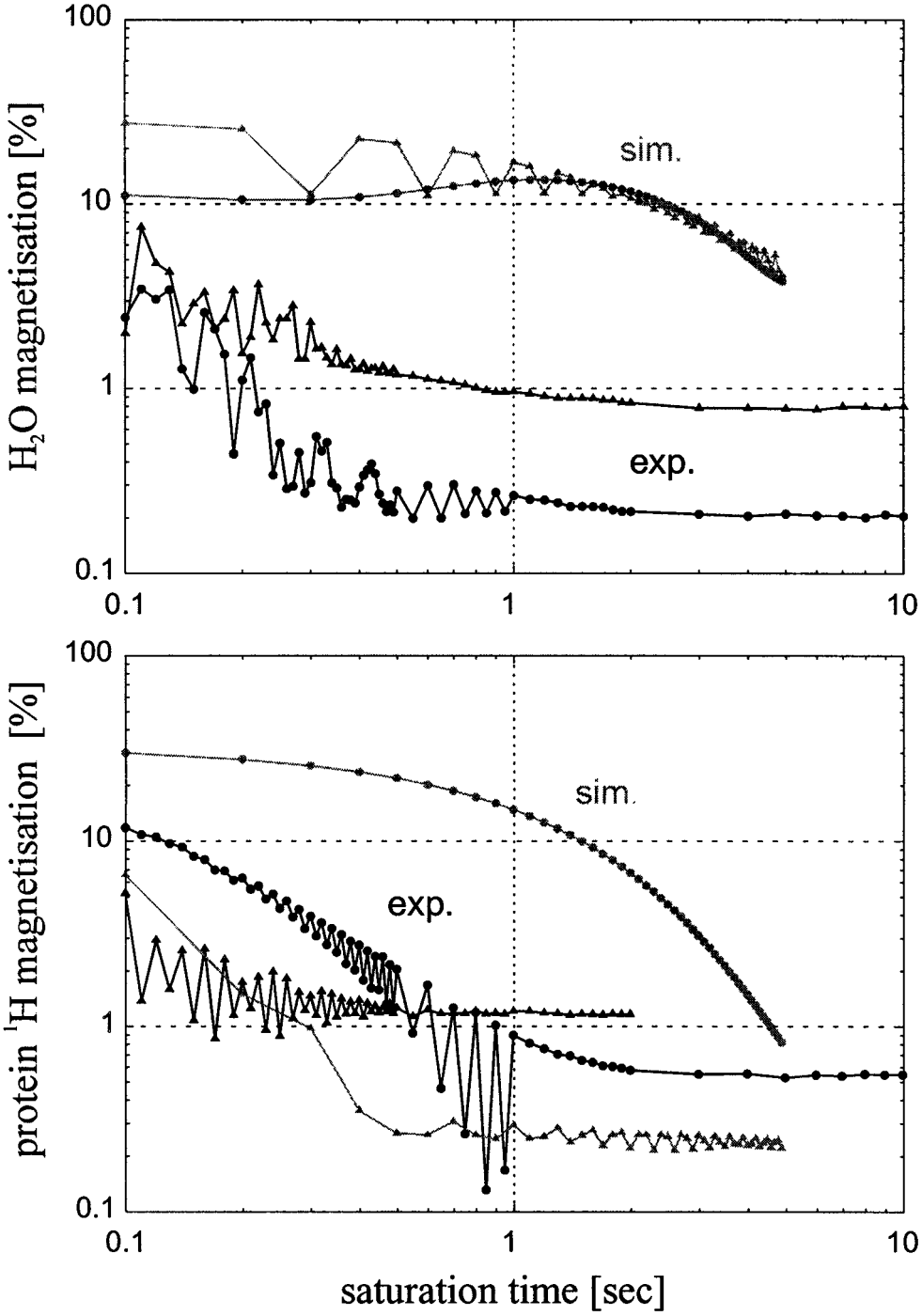

Figure 2. Saturation of proton magnetisation (top: water, bottom: protein) with 120° pulse trains (triangles) and 188° pulse trains (filled circles). The saturation period followed a relaxation delay of 1 s. In grey simulation results are included. In the simulations 120° pulses (triangles) and perfect 180° pulses (circles) were used. Note the logarithmic scale on both axes.

simulation in the saturation curves for water magnetisation derive from the fact that radiation damping could not be included in the simulations. Apparently radiation damping is the main mechanism by which water magnetisation is saturated. For protein magnetisation very different saturation curves are obtained in the simulations with 120° and 180° saturation pulses. It is clear that applying perfect 180° pulses on an on-resonant single spin leads only to signal reduction via T_1 relaxation and that T_2 relaxation, which is much faster for the protein, does not help in saturating the proton magnetisation. These simulation results show that it is not desirable to use exact 180° pulses. The 188° pulses used in our experiments were found to perform best in saturating water magnetisation (0.2% residual water magnetisation compared to 0.8% for the 120° pulses and 0.7% for 250° pulses). The saturation of protein magnetisation with 188° pulses proceeds slower than with 120° pulses in the very beginning, but is more efficient for all saturation times longer than one second. The fact that in the simulations a lower residual protein magnetisation is observed using 120° pulses for long saturation times than in the experiment may be attributed to absence of neighbouring and interacting spins in the simulations. Additional experiments with different delays (5 ms, 10 ms and 20 ms) between pulses during the saturation period showed that for 120° pulses a longer delay is preferable (20 ms), whereas for 180° the shortest delay (5 ms) performed best, albeit at increased sample heating. We used 10 ms delays between saturation pulses for all experiments shown in Figure 2 and also for the mapping of saturation in the NOE experiment with proton saturation depicted in Figure 3. NOE curves of Figure 3 for rigid and for flexible residues were obtained by integration of signals with amide proton shifts downfield from 8.5 ppm (= rigid) and between 8.5 ppm and 8.1 ppm (= flexible). Between 8.5 ppm and 8.1 ppm mostly flexible and disordered residues resonate, whereas above 8.5 ppm only residues of the rigid core of the protein occur (Fucini et al., 1997). Again 188° pulses and 120° pulses were similarly efficient, with the 188° pulses resulting in slightly better saturation. NOE saturation experiments were performed with 1s relaxation delay before the saturation period or with only 100 ms relaxation delay. The latter experiments required longer saturation times; however, the overall time per scan is reduced by 0.9 s. This leads to more efficient saturation of flexible residues, but less efficient saturation of rigid residues. Remarkably, for rigid residues in our protein incomplete T_1 relaxation during a 1s relaxation delay almost exactly cancels with incomplete saturation for short saturation periods, such that for all saturation times the final NOE value of ~0.7 is obtained in the NOE experiments (Figure 3, top black curves). 250° pulses displayed saturation behaviour in all experiments and simulations very similar to 120° pulses, and are therefore not included in Figures 2 and 3.

Relaxation in the NOE reference experiment

Figure 4 shows the dependence of signal intensity on the relaxation delay in the NOE reference experiment. Curves for flexible and rigid residues are obtained as before (*vide supra*). Data points from full 2D het-NOE reference experiments are included in Figure 4 (squares and diamonds). The importance of using the water flip-back technique is immediately evident. Without water flip-back even negative signals are observed in the reference experiment for short relaxation delays (Figure 4, open diamonds). These data points are reproduced by the analytical expression valid for fast exchange of amide protons with saturated water and for instantaneous equilibrium between cross relaxation between amide proton and nitrogen and T_1 relaxation of the ^{15}N nitrogen (Skelton et al., 1993): $I_{exp}/I_{true} = 1 - (1 - NOE)\exp(-t/T_1^{water})$. The T_1 of water was determined for the present sample and at 31° as 3.4 s.The NOE of the very flexible residues is approx. −1. Thus the broken blue line in Figure 4 is derived: $I_{rel} = I_{exp}/I_{true} = 1 - 2\exp(-t/3.4\ s)$. With water flip-back we found that 80% of the water magnetisation is preserved at the end of a scan. Therefore less saturation is transferred to the protein. In the steady state the loss of 20% of the water magnetization during a single scan must be exactly balanced by the T_1 relaxation during the relaxation delay between scans. From this follows an expression for the fraction of water magnetisation that is saturated for a given relaxation delay t: $I_{sat}/I_0 = 1 - (1 - \exp(-t/T_1^{water}))/(1 - 0.8\exp(-t/T_1^{water}))$. Thus, the broken red line of Figure 4 is derived for very flexible residues (NOE = −1) in fast exchange with water and instantaneous equilibrium between cross relaxation and ^{15}N T_1 relaxation (see above). It agrees nicely with the corresponding experimental data points (Figure 4, grey filled diamonds). Obviously, in the regime of high flexibility and for medium to long relaxation times saturation transfer from water to the amide protons is the most important factor. For rigid residues that do not exchange with water incomplete T_1 relaxation

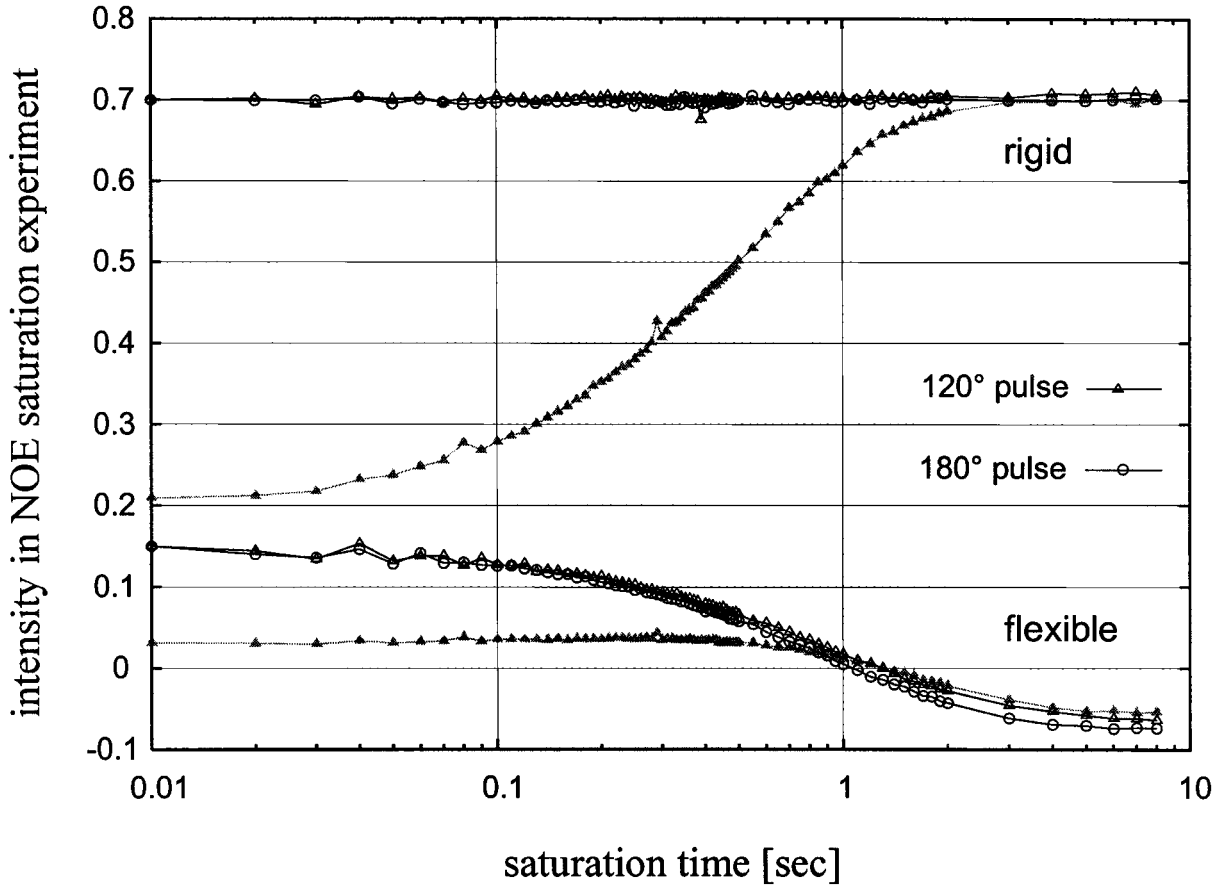

Figure 3. Relative intensity in the NOE experiment with proton saturation. Saturation of proton magnetisation was achieved by 120° pulse trains (triangles) and 188° pulse trains (circles). For the black curves a relaxation delay of 1 s preceded the saturation period, for the grey curves only 0.1 s relaxation was used. The signal intensities were scaled relative to an experiment with no proton saturation and very long relaxation delay (20 s). For definition of rigid and flexible see text. Note the logarithmic scale on the abscissa (saturation time).

of the amide proton is still determining the signal intensity for long relaxation delays. The corresponding analytical expression is given by $I_{rel} = I_{exp}/I_{true} = 1 - (1 - NOE)\ exp(-t/T_1^H)$ (Grzesiek and Bax, 1993). In our case for amide protons average values of $T_1^H = 1.3$ s and NOE = 0.7 were found for residues of the folded core (1–100). This yields $I_{rel} = 1 - 0.3\ exp(-t/1.3\ s)$ (Figure 4, broken line in magenta). For the flexible residues the average NOE value is approx. −0.1 as seen from Figure 3. The broken green curve in Figure 4, that corresponds to the data points for flexible residues (triangles), is therefore given by $I_{rel} = 1 - 1.1\ exp(-t/1.3\ s)$. For short relaxation times it is clear that T_1 relaxation of the ^{15}N and cross relaxation between proton and nitrogen have to be considered. The experimental values for flexible and rigid residues at short and very short relaxation times are not reproduced by the analytical expressions described above.

A simplified way of taking into account the role of ^{15}N T_1 relaxation consists of multiplying above equations by a term $1 - exp(-t/T_1^N)$. Here the average T_1^N is 450 ms (Renner et al., 2000). This yields the solid curves of Figure 4, which are in qualitative agreement with the experimental data points. Obviously, for flexible residues the difference is small, whereas for rigid residues a big improvement is achieved. For a rigorous theoretical treatment the coupled differential equations for all participating nuclei have to be solved. However, this requires detailed knowledge of all motional parameters (Skelton et al., 1993) and is therefore not useful for an estimation of error in advance.

From Figures 3 and 4 an expected systematic error can be estimated for given saturation and relaxation periods. For example, taking the red curve of

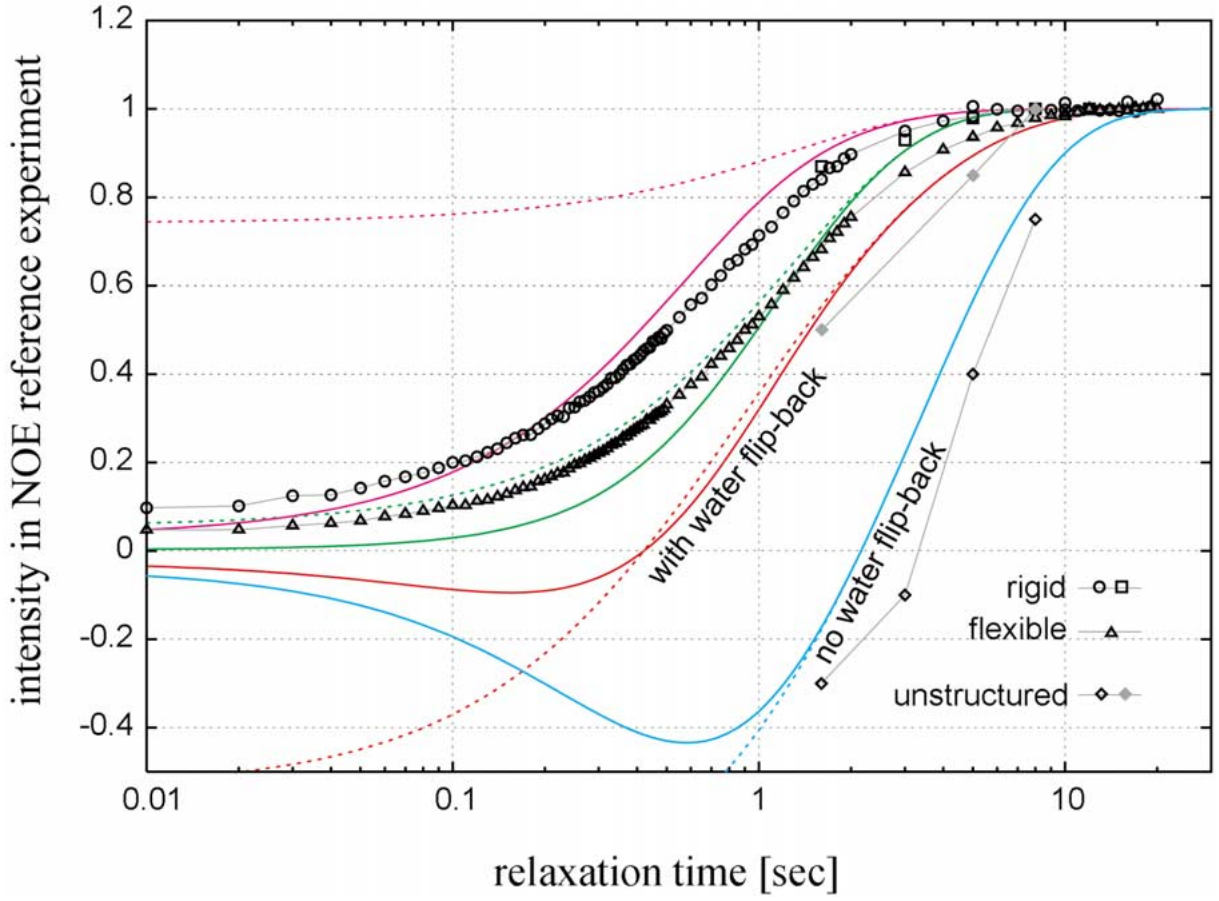

Figure 4. Relative Intensity in the NOE reference experiment. Data points were determined from full 2D NOE experiments (squares and diamonds) or from pseudo 2D experiments (circles and triangles). Coloured broken and solid curves correspond to analytical expressions derived from simple models (see text). Broken lines correspond to the limit of long relaxation times; solid lines take into account ^{15}N T_1 relaxation. From top to bottom: (a) incomplete T_1 relaxation of the amide proton for rigid residues (NOE $\sim$ 0.7) (magenta); (b) the same for flexible residues (NOE ~ -0.1) (green); (c) saturation transfer from moderately saturated water magnetisation (water flip-back technique) to very flexible amide protons (red); (d) saturation transfer from saturated water (no water flip-back) to very flexible amides (blue). Note the logarithmic scale on the abscissa (relaxation time).

Figure 1 with 1.6 s relaxation delay and 1.5 s saturation period (with only 100 ms relaxation preceding the saturation period) one finds from Figure 3 (grey triangles, top curve) that for rigid residues 4% underestimation are to be anticipated from incomplete T_1 relaxation in the NOE saturation experiment. From Figure 4 (open circles) incomplete relaxation in the reference experiment is expected to result in 16% underestimation of the reference intensity. The combined effect should be hetNOE values 1.14 times too large ($0.96/0.84 = 1.14$). Experimentally, hetNOE values for folded residues were on average 19% too high. For the hetNOE values recorded with 3s saturation and 3.1 s relaxation (blue curve in Figure 1) no appreciable error is expected due to incomplete saturation. However, Figure 4 indicates that incomplete relaxation should result in 7% overestimation, in good agreement with the 6% error observed experimentally. Somewhat unclear is why the combination of 1 s saturation/5 s relaxation performs so badly (hetNOE for the folded core overestimated by 14%). Incomplete relaxation contributes negligibly to the systematic error as is clearly seen from Figure 4. Apparently, the long relaxation time of 4 s that precedes the short saturation time of 1 s leads to significantly incomplete saturation even for the rigid residues. Figure 3 indicates that by reducing the relaxation time before the saturation period to 1 s accurate values for the hetNOE should be obtained, shortening the experimental time simultaneously. For flexible residues prediction of errors is

more difficult. Figures 3 and 4 provide guidelines how flexible residues behave, but cannot contain curves for every degree of flexibility possible. Still, the two lowest curves of Figure 4 (open and filled diamonds) can be considered the 'worst case' scenario (completely disordered residues in fast exchange with water).

Finally, the influence of molecular size on the systematic errors in the NOE experiments as discussed above shall be addressed. For unstructured residues chemical exchange with saturated water is the major source of error and therefore molecular size plays (almost) no role. For less flexible residues estimation of amide proton and nitrogen T_1 allows for calculation of curves analogous to that of Figure 4. The main effect is a shift of the curves to the right for larger proteins (longer amide proton T_1) and to the left for smaller proteins (shorter T_1) compared to the model system presented here.

Conclusions

From the results presented here it can be concluded that the accuracy of NOE measurements depends strongly on the flexibility of the given amino acid. Therefore, an a priori decision should be made regarding the extent of quantitative analysis that is intended. For qualitative assessment of a protein's dynamic or identification of folded, flexible and unstructured parts relaxation delays as short as 1.5 s may be chosen. In this case no NOE value should be calculated for amino acids where the peak intensity in the NOE experiment is negative. These residues can only be classified as disordered without further quantification. On the other hand, if one aims at quantifying large amplitude motions correctly, relaxation delays definitely longer that the commonly used 5 s must be chosen. The present study indicates that a relaxation delay of 10 s is sufficient for all degrees of flexibility observable in structured parts of proteins. For completely unstructured residues an even longer delay of 20 s needs to be employed to allow full relaxation of the water magnetisation. Highly accurate NOE measurements also require full saturation of all protons including water. A new saturation sequence consisting of approximate 180° pulses was shown to perform slightly better in fully saturating proton magnetization than the commonly used 120° pulses. For saturation the time requirements are lower. After 5 s of saturation the maximum saturation is reached. A relaxation delay of 1 s preceding the saturation period allows much faster saturation (< 1 s) of amino acids with limited flexibility.

Supporting information

Tables listing all NOE values are available from the authors.

Acknowledgements

The authors thank Paola Fucini for preparing the ^{15}N-labeled protein sample. Helpful comments, careful reading and constructive criticism from two anonymous referees are gratefully acknowledged. This work was supported by SFB 533 (C.R. and L.M.) and SFB 413 (M.S. and T.A.H.) of the Deutsche Forschungsgemeinschaft.

References

Bronstein, I.N. and Semendjajew, K.A. (1957) *Taschenbuch der Mathematik*, Teubner, Leipzig.

Buck, M., Schwalbe, H. and Dobson, Ch.M. (1996) *J. Mol. Biol.*, **257**, 669–683.

Cieslar, C., Ross, A., Zink, T. and Holak, T.A. (1993) *J. Magn. Reson.*, **101**, 97–101.

Clore, G.M., Driscoll, P.C., Wingfield, P.T. and Gronenborn, A.M. (1990) *Biochemistry*, **27**, 7387–7401.

Dayie, K.T., Wagner, G. and Lefèvre, J.-F. (1996) In *Dynamics and the Problem of Recognition in Biological Macromolecules* Jardetzky, O. and Lefèvre, J.-F. (Eds.), NATO ASI Series A, Vol. 288, Plenum Press, New York, NY.

Farrow, N.A., Muhandiram, R., Singer, A.U., Pascal, S.M., Kay, C.M., Gish, G., Shoelson, S.E., Pawson, T., Foreman-Kay, J.D. and Kay, L.E. (1994) *Biochemistry*, **33**, 5984–6003.

Fischer, M.W.F., Majumdar, A. and Zuiderweg, E.R.P. (1998) *Prog. NMR Spectrosc.*, **33**, 207–272.

Fucini, P., Renner, C., Herberholt, C., Noegel, A.A. and Holak, T.A. (1997) *Nat. Struct. Biol.*, **4**, 223–230.

Fushman, D., Cahill, S. and Cowburn, D. (1997) *J. Mol. Biol.*, **266**, 173–194.

Fushman, D., Tjandra, N. and Cowburn, D. (1999) *J. Am. Chem. Soc.*, **121**, 8577–8582.

Grzesiek, S. and Bax, A. (1993) *J. Am. Chem. Soc.*, **115**, 12593–12594.

Kay, L.E. (1998) *Biochem. Cell Biol.*, **76**, 145–152.

Kay, L.E., Torchia, D.A. and Bax, A. (1989) *Biochemistry*, **28**, 8972–8979.

Lefèvre, J.-F., Dayie, K.T., Peng, J.W. and Wagner, G. (1996) *Biochemistry*, **35**, 2674–2686.

Li, Y.-C., Montelione, G.T. (1994) *J. Magn. Reson.*, **B105**, 45–51.

Markley, J.L., Horsley, W.J. and Klein, M.P. (1971) *J. Chem. Phys.*, **55**, 3604–3605.

Mühlhahn, P., Zweckstetter, M., Georgescu, J., Ciosto, C., Renner, C., Lanzendörfer, M., Lang, K., Ambrosius, D., Baier, M., Kurth, R. and Holak, T.A. (1998) *Nat. Struct. Biol.*, **5**, 682–686.

Orekhov, V.Y., Pervushin, K.V., Korzhnev, D.M. and Arsieniev, A.S. (1995) *J. Biomol. NMR*, **6**, 113–122.

Palmer, A.G. (1997) *Curr. Opin. Strut. Biol.*, **7**, 732–737.

Papavoine, C.H.M., Remerowski, M.L., Horstink, L.M., Kronings, R.N.H., Hilbers, C.W. and van der Ven, F.J.M. (1997) *Biochemistry*, **36**, 4015–4026.

Peng, J.W. and Wagner, G. (1992) *Biochemistry*, **31**, 8571–8586.

Renner, C.and Holak, T.A. (2000) *J. Magn. Reson.*, **145**, 192–200.

Renner, C. and Holak, T.A. (2001) *Eur. J. Biochem.*, **268**, 1058–1065.

Renner, C., Baumgartner, R., Noegel, A.A. and Holak, T.A. (1998) *J. Mol. Biol.*, **283**, 221–229.

Skelton, N.J., Palmer III, A.G., Akke, M., Kördel, J., Rance, M. and Chazin, W.J. (1993) *J. Magn. Reson.*, **B102**, 308–332.

Smith, G.M., Yu, L.P. and Domingues, D.J. (1987) *Biochemistry*, **26**, 2202–2207.

Tessari, M., Mulder, F.A.A., Boelens, R. and Vuister, G.W. (1997) *J. Magn. Reson.*, **127**, 128–133.

Tjandra, N., Szabo, A. and Bax, A. (1996) *J. Am. Chem. Soc.*, **118**, 6986–6991.

Viles, J.H., Donne, D., Kroon, G., Prusinger, S.B., Cohen, F.E., Dyson, H.J. and Wright, P.E. (2001) *Biochemistry*, **40**, 2743–2753.

Zheng, Z., Czaplicki, J. and Jardetzky, O. (1995) *Biochemistry*, **34**, 5212–5223.

Zink, T., Ross, A., Lüers, K., Cieslar, C., Rudolph, R. and Holak, T.A. (1994) *Biochemistry*, **33**, 8453–8463.